



Pore Pressure Generation of Gravelly Soils in Constant Volume Cyclic Simple Shear

Jonathan F. Hubler, A.M.ASCE¹; Adda Athanasopoulos-Zekkos, M.ASCE²; and Dimitrios Zekkos, P.E., M.ASCE³

Abstract: Excess pore pressure generation of uniform gravel and gravel-sand mixtures was evaluated in this study. Comparisons were made with existing relationships for pore pressure generation of sands and show that gravel and gravel-sand mixtures can exhibit different pore pressure responses. The influence of liquefaction definition, gravel particle angularity, particle size, relative density, initial vertical effective stress, cyclic stress ratio, and gravel percentage, on the generation of excess pore water pressure of gravel and gravel-sand mixtures was studied. Liquefaction definition, particle size, initial vertical effective stress, and cyclic stress ratio were found to not have a significant effect on the normalized excess pore pressure generation (i.e., r_u versus N/N_L). Conversely, relative density, particle angularity, and mixture percentage of gravels were found to have a more significant effect on the normalized excess pore pressure generation response (i.e., r_u versus N/N_L). Additionally, the coefficient of uniformity (C_u) was found to have a strong correlation with increased excess pore pressure generation ratio at values of N/N_L less than 0.40, highlighting the influence of grain size distribution on early pore pressure generation response. A new pore pressure model was developed to predict r_u based on C_u for gravelly soils. **DOI:** 10.1061/(ASCE)GT.1943-5606.0002928. © 2022 American Society of Civil Engineers.

Author keywords: Pore pressure generation; Gravelly soils; Cyclic simple shear.

Introduction

Excess pore pressure generation during undrained cyclic loading is critical in understanding the response of soils during earthquakes. During undrained loading, excess pore pressures develop due to the tendency of material to contract during shearing, which causes a reduction in effective confining stress and therefore a loss of stiffness. The buildup of pore pressure may lead to soil liquefaction. Pore pressure buildup has been studied utilizing laboratory element tests in sands (Lee and Albaisa 1974; De Alba et al. 1975; Martin et al. 1975; Seed et al. 1975; Dobry et al. 1982; Kammerer et al. 2004; Wu et al. 2004), and silt and sand-silt mixtures (Green et al. 2000; Polito and Martin 2001; Polito et al. 2008; Porcino and Diano 2016), but limited data is available for gravelly soils (Banerjee et al. 1979; Evans and Seed 1987; Hynes 1988; Haeri and Shakeri 2010; Chang et al. 2014; Hubler et al. 2017b). Additionally, the effects of several parameters, including vertical effective stress, applied stresses, particle angularity, and coefficient of uniformity (C_u) , require further study to fully evaluate their influence on pore pressure generation of gravelly soils.

¹Assistant Professor, Dept. of Civil and Environmental Engineering, Villanova Univ., 800 Lancaster Ave., Villanova, PA 19085 (corresponding author). ORCID: https://orcid.org/0000-0002-0145-1036. Email: jonathan.hubler@villanova.edu

²Associate Professor, Dept. of Civil and Environmental Engineering, Univ. of California, Berkeley, 421 Davis Hall, Berkeley, CA 94720. ORCID: https://orcid.org/0000-0002-3785-9009. Email: adda.zekkos@berkeley.edu

³Professor, Dept. of Civil and Environmental Engineering, Univ. of California, Berkeley, 425 Davis Hall, Berkeley, CA 94720. ORCID: https://orcid.org/0000-0001-9907-3362. Email: zekkos@berkeley.edu

Note. This manuscript was submitted on March 7, 2021; approved on August 10, 2022; published online on December 1, 2022. Discussion period open until May 1, 2023; separate discussions must be submitted for individual papers. This paper is part of the *Journal of Geotechnical and Geoenvironmental Engineering*, © ASCE, ISSN 1090-0241.

Excess pore pressure generation of sands can be predicted using empirical models developed from laboratory testing. Seed et al. (1975) developed a stress-based model using data from undrained, stress-controlled cyclic triaxial tests on sand. Eq. (1) shows the empirical model that was developed using the relationship between the excess pore pressure ratio $\{r_u = [(u_{excess})/(\sigma'_{v0})]\}$ defined as the ratio of excess pore pressure u_{excess} to initial vertical effective stress σ'_{v0} , and the cyclic ratio (N/N_L) , which is the number of cycles normalized by the number of cycles to liquefaction

$$r_u = \frac{1}{2} + \frac{1}{\pi} \arcsin\left(2 \times \left(\frac{N}{N_L}\right)^{1/\alpha} - 1\right) \tag{1}$$

where α is an empirical constant that is a function of the soil properties and test conditions. An α value of 0.70 was found to best fit the sand data in Seed et al. (1975). Booker et al. (1976) developed an alternative, simplified version:

$$r_u = \frac{2}{\pi} \arcsin\left(\frac{N}{N_I}\right)^{\frac{1}{2\beta}} \tag{2}$$

where β is a parameter that changes the shape of the excess pore pressure generation versus N/N_L curve. A higher value of β increases the excess pore pressure generation at lower ratios of N/N_L . A value of $\beta=0.70$ was recommended for clean sands (Booker et al. 1976). Other models for excess pore pressure generation exist that are stress-based (Polito et al. 2008), strain-based (Martin et al. 1975; Dobry et al. 1985), and energy-based (Berrill and Davis 1985; Green et al. 2000; Kokusho 2013).

Current models for excess pore pressure generation have all been developed using laboratory test data for sandy and silty soils. The effect of adding finer particles to sand has been studied and it has been shown that pore pressure response can be different than the sand relationship from Lee and Albaisa (1974) when silt is added (Polito 1999; Porcino and Diano 2016). However, the effect of adding larger gravel particles to sand is far less

investigated due to the unavailability of large-size laboratory devices that can accurately capture the pore pressure generation of gravelly soils. Additionally, many of the laboratory studies that have been performed for gravelly soils have utilized cyclic triaxial testing, which requires corrections for membrane compliance effects. Membrane compliance effects have been studied for gravels (Evans and Seed 1987; Haeri and Shakeri 2010); however, there is not an agreed upon method for applying membrane corrections.

Existing gravel studies have generally found that the excess pore pressure generation response of gravels and gravelly soils is different than that of sands. Banerjee et al. (1979) performed large-size cyclic triaxial tests on well-graded Oroville gravel with a maximum particle size of 5 cm (2") and found excess pore pressure generation for gravels increased rapidly in the first few cycles and then slowly in the subsequent cycles. Wong et al. (1974) reported similar results for well-graded Oroville gravel. Evans and Seed (1987) tested gravel in a large-size triaxial apparatus (307 mm diameter) and a smaller-size triaxial apparatus (71 mm diameter), and sluiced the specimens with sand to minimize the effects of membrane compliance. The authors compared unsluiced (compliant) and sluiced specimens (i.e., sluiced with sand to fill the peripheral voids of the specimen) and found that unsluiced specimens had a cyclic resistance that was 55% higher and displayed a different pore pressure generation response. Sluiced specimens were noted to generate more reliable excess pore pressures, which fell near the upper bound of the Lee and Albaisa (1974) data for sand. Hynes (1988) performed large-size triaxial tests on Folsom gravel and found pore pressure generation at cyclic shear strain levels of 1% to be independent of initial confining stress, relative density, overconsolidation ratio, and anisotropic consolidation conditions. Chang et al. (2014) presented cyclic simple shear data for the liquefaction response of gap-graded gravelly soils and found pore pressure generation to increase with increasing gravel content to levels that were similar to or below that of sands.

Several studies have also investigated the excess pore pressure generation during monotonic and cyclic testing of sand and silt mixtures, which can offer some insight into the gravel mixture response. Belkhatir et al. (2014) performed undrained monotonic triaxial tests on sand-silt mixtures to study the effect of gradation on pore pressure generation. Results showed that the maximum excess pore pressure decreased with an increase of D_{10} and D_{50} , while it increased with an increase in C_u and fines content. Belkhatir et al. (2014) also observed that as the silt fraction increased in the mixture, the maximum excess pore pressure increased gradually. Dash and Sitharam (2009) studied the undrained cyclic response of sandsilt mixtures by performing stress-controlled triaxial tests. The authors found that pore pressure generation was greatly influenced by the limiting silt content and relative density of the specimen. At very high relative densities (greater than 70%), pore pressure response and cyclic resistance were found to be independent of silt content. Polito (1999) studied the effect of fines on the cyclic pore pressure generation of non-plastic silt when added to sand using triaxial tests, and found that the generation of pore pressure was insensitive to relative density, cyclic stress ratio, and silt content. Polito (1999) recommended that separate curves of excess pore pressure generation versus N/N_L are necessary for soils susceptible to flow liquefaction compared to soils that exhibit cyclic mobility. The sand and sand-silt specimens exhibiting cyclic mobility generated greater excess pore pressure at lower values of N/N_L than specimens with flow liquefaction. Porcino and Diano (2016) performed cyclic simple shear tests on clean sand, sand with silt (silt contents up to 39%), and sandy silt (silt content of 62%). Those mixtures had C_u values that ranged from 2.8 to 24. Porcino and Diano (2016) also found that the normalized curves for excess pore pressure generation for silty sands did not follow the trends for clean sands. These studies of silt and sand-silt mixtures showed that existing pore pressure models for sands may not fit the response of silt and silt-mixtures, as the gradation of these materials influenced cyclic shear response and therefore the pore pressure generation response. Additionally, Mei et al. (2018) found that the coefficient of uniformity (C_u) had a significant influence on the pore water pressure generation of sands with C_u of 1.4–3.7, and updated the Vucetic and Dobry (1986) pore water pressure model to account for these changes.

Existing literature on sand and sand-silt mixtures shows that pore pressure generation is dependent on C_u ; however, this relationship has not been explored for gravelly soils. It is hypothesized that the pore pressure generation of gravelly soils is different from that of poorly-graded sands and will exhibit a dependency on C_u . In this study, a large-size cyclic simple shear (CSS) device was utilized to perform cyclic shear tests of gravel, sand, and gravel-sand mixtures, with an emphasis on evaluating the effects of particle angularity of gravel, liquefaction definition, relative density, initial vertical effective stress, cyclic stress ratio, and gravel percentage for gravel-sand mixtures, on the generation of excess pore water pressure. Relationships of excess pore pressure generation with C_u are explored to test the research hypothesis.

Test Materials

The materials tested in this study included both uniform sand and gravel as well as gap-graded mixtures of gravel and sand. The uniform materials included Ottawa C109 sand, pea gravel (PG), 5 mm crushed limestone (CLS5), and 8 mm crushed limestone (CLS8). Mixtures of Ottawa C109 sand with either pea gravel or CLS8 were tested with mixture percentages of 80% sand/20% gravel, 60% sand/40% gravel, and 40% sand/60% gravel. Grain size distributions for all tested materials are shown in Fig. 1. Discussion of the uniform materials can be found in Hubler et al. (2017a), and discussion of the gravel-sand mixtures can be found in Hubler et al. (2018). The uniform gravels were selected because of their varying particle morphology. The pea gravel is subrounded, while the crushed limestone gravels are both angular, but with different particle sizes. The Ottawa C109 sand is subrounded with a $D_{50} =$ 0.35 mm. The properties of these various materials are listed in Table 1, and their coefficients of uniformity, coefficients of curvature, and D_{50} values are given in Table 2. Similar to sand and silt mixtures where a transition zone from sand- to silt-dominated response is typically in the 20%-35% silt range (Lade et al. 1998; Cubrinovski and Ishihara 2002; Polito and Sibley 2020), the minimum and maximum void ratios of the gravel-sand mixtures tested in this study decrease to a local minimum at approximately 40%-60% gravel content. Gravel-sand mixtures with 40%-60% gravel were subsequently found to exhibit the highest strength and resistance to liquefaction. Below this transition zone (i.e., mixtures with greater sand percentage), responses became more sand dominated. Additionally, the particle morphology of the mixing gravel was shown to be an important factor in overall response (Hubler et al. 2018).

Test Procedure

A CSS device was utilized in this study to perform cyclic tests on uniform gravels and gravel-sand mixtures. The specimen diameter was 307.5 mm and the specimen was laterally confined by stacked rings. The CSS device was described in detail by Zekkos et al. (2018).

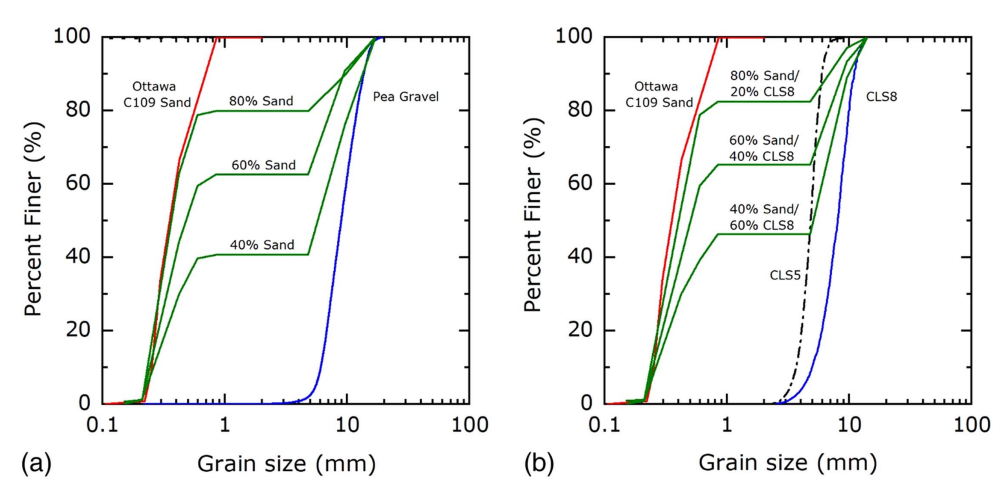


Fig. 1. Grain size distribution curves for (a) pea gravel and pea gravel Ottawa sand mixtures; and (b) CLS5, CLS8, and CLS8 and Ottawa sand mixtures.

Table 1. Properties of test materials

Materials	G_S	$\gamma_{ m d,max} \ ({ m kg/m^3})$	$\gamma_{ m d,min} \ ({ m kg/m^3})$	e _{max}	e _{min}
Pea gravel	2.74	1,741	1,546	0.772	0.574
8 mm crushed limestone	2.65	1,751	1,357	0.953	0.513
5 mm crushed limestone	2.65	1,667	1,276	1.077	0.590
Ottawa C109 sand	2.65	1,733	1,512	0.752	0.529
60% pea gravel/40% sand	2.70	2,114	1,960	0.379	0.279
40% pea gravel/60% sand	2.69	1,978	1,818	0.477	0.358
20% pea gravel/80% sand	2.67	1,848	1,665	0.602	0.443
60% CLS8/40% sand	2.65	2,223	2,068	0.419	0.313
40% CLS8/60% sand	2.65	2,032	1,842	0.455	0.335
20% CLS8/80% sand	2.65	1,870	1,660	0.586	0.413

Table 2. Coefficient of uniformity, coefficient of curvature, and d_{50} values for materials used in model development

				D_{50}
Source	Material	C_u	C_c	(mm)
Banerjee et al. (1979)	Gravel	47	3.85	9.53
Evans and Seed (1987)	Gravel	1.3	1.03	6.00
Hynes (1988)	Gravel	14	3.00	22.2
Haeri and Shakeri (2010)	Gravelly sand	28	1.80	4.00
Pea gravel	Gravel	1.6	0.90	9.00
CLS5	Gravel	1.4	1.00	4.85
CLS8	Gravel	1.7	1.10	8.00
80% sand/20% PG	Sand-gravel mix	1.8	1.67	0.37
60% sand/40% PG	Sand-gravel mix	2.6	0.82	0.49
40% sand/60% PG	Sand-gravel mix	26	0.10	5.84
80% sand/20% CLS8	Sand-gravel mix	2.2	0.90	0.40
60% sand/40% CLS8	Sand-gravel mix	2.4	0.62	0.50
Porcino and Diano (2016)	Sand with silt	4	1.48	0.08
Porcino and Diano (2016)	Sandy silt	24	2.67	0.10
Porcino and Diano (2016)	Sandy silt	17	4.05	0.03
Porcino and Diano (2016)	Clean sand	2.8	1.49	0.32

Specimens were prepared in loose ($D_r = 47\%$) and dense ($D_r = 87\%$) states. Loose specimens were prepared by dry pluviation with a funnel or by using a small scoop, while the dense specimens were prepared by dry pluviation or a small scoop in layers and using a 5.5 kg drop weight to densify to a target density. Minimum density

was evaluated by using a small scoop or funnel for the uniform sand and gravels as well as the gravel-sand mixtures (ASTM 2016). Maximum density was evaluated for the uniform sand and gravels using a vibratory table (ASTM 2016); however, gravel-sand mixtures exhibited segregation during vibratory table maximum density trials. A method was developed to achieve the maximum density for gravelsand mixtures and compared with prediction equations developed by Fragaszy and Sneider (1991). The method, as summarized in Hubler et al. (2017a), utilized the same mold used in the vibratory table testing and consisted of placing mixtures in 25 mm lifts, tamping the mold with a rubber mallet 25 times, and tamping the surface 100 times with a small cylinder. This method resulted in values for maximum density that compared favorably to the prediction equation (Fragaszy and Sneider 1991), as well as for mixtures at 80% sand/ 20% gravel that were tested using the vibratory table (ASTM D4254). The 80% sand/20% gravel specimens did not exhibit segregation in the vibratory table and therefore served as a reference point for the new method. Further information on specimen preparation can be found in Hubler et al. (2017a, 2018).

Cyclic simple shear tests were performed using the CSS device where liquefaction was defined as the attainment of 3.75% single amplitude shear strain, which is commonly used in cyclic simple shear testing (Vaid and Sivathayalan 1996; Sivathayalan 2000; Porcino and Diano 2016). The excess pore pressure ratio (r_u) at this shear strain ranged from approximately 0.80 to 1, depending on the test specimen, as discussed in subsequent sections. Test specimens were first consolidated to the desired vertical stress, which ranged from 50 to 400 kPa, and then cyclically sheared under stress-controlled conditions. Cyclic stress ratios (CSR) ranging from 0.04 to 0.14 at a loading frequency of 0.33 Hz were applied to the specimens. All cyclic tests were performed at constant volume conditions, which have been shown to accurately represent truly undrained conditions in simple shear testing (Dyvik et al. 1987). In constant volume simple shear testing, the measured change in the vertical stress is assumed to be equal to the pore pressures that would develop in a truly undrained test. Constant volume conditions were maintained in the CSS device by active control through a feedback loop, which suppresses movement of the vertical cap and allows for accurate measurement of the change in vertical stress, thus limiting the vertical strain to less than 0.05%, which is the threshold used in ASTM D8296 (ASTM 2019) for constant volume cyclic simple shear testing.

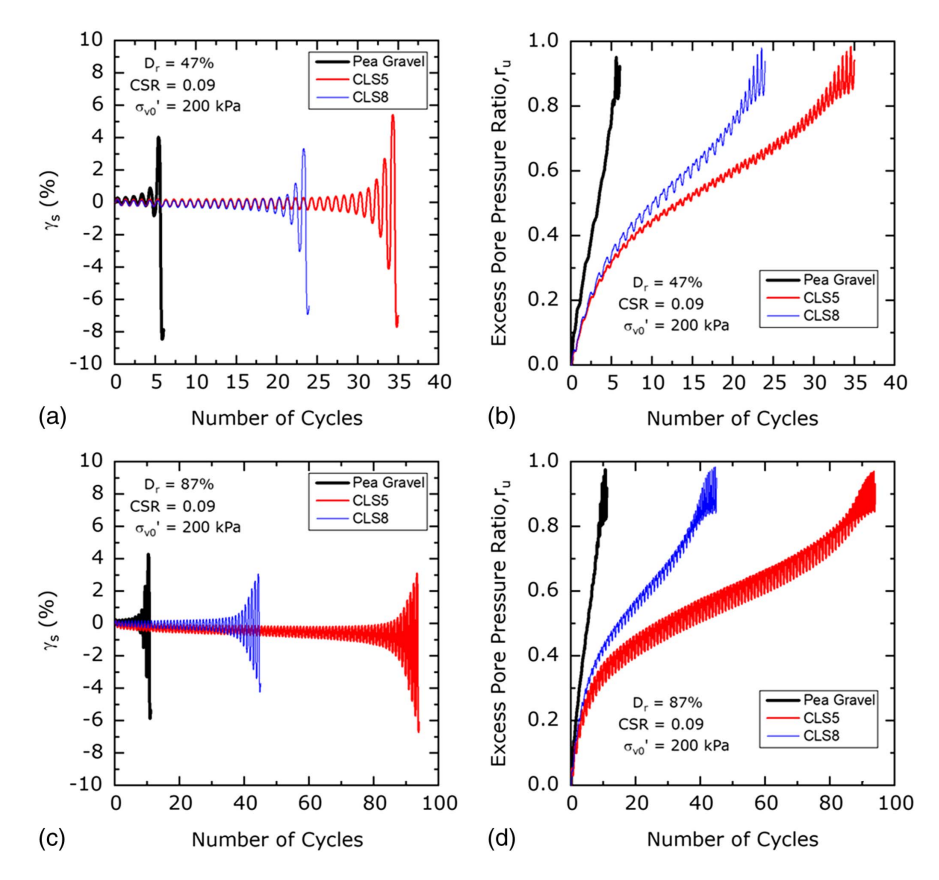


Fig. 2. Cyclic shear data for pea gravel, CLS5, and CLS8 at $\sigma'_{vo} = 200$ kPa, CSR = 0.09 for (a) shear strain versus number of cycles for $D_r = 47\%$; (b) excess pore pressure ratio versus number of cycles for $D_r = 47\%$; (c) shear strain versus number of cycles for $D_r = 87\%$; and (d) excess pore pressure ratio versus number of cycles for $D_r = 87\%$.

Results

Data from cyclic liquefaction tests are presented in this section to evaluate both uniform gravels and the effect of gravel percentage within a gravel-sand mixture on excess pore pressure generation response. Mixtures were tested at loose ($D_r = 47\%$) and dense $(D_r = 87\%)$ conditions at vertical effective stresses ranging from 50 to 400 kPa. Tests are compared at global relative densities of the gravel-sand mixtures, and relationships between particle angularity, gradation, and mixture percentage are explored. Evans and Zhou (1995) noted that gravel-sand mixtures with varying gravel contents cannot be compared at identical composite void ratios, as the minimum and maximum void ratios may not be achievable for certain mixtures. Therefore, to enable comparison at different gravel-sand mixture compositions, relative density was used as the comparison metric. Example data for the uniform gravels at $D_r =$ 47% and $D_r = 87\%$, at an initial vertical stress of 200 kPa and a CSR of 0.09, are shown in Fig. 2. The stress-strain response and corresponding excess pore pressure generation ratio (r_u) data is presented and shows distinct differences between the gravels, with both particle angularity and relative density influencing response. The more angular CLS materials generate pore pressure at a much slower rate than the rounded pea gravel. The larger size CLS8 material liquefies in approximately 10 fewer cycles than the CLS5 material. An increase in D_r increases the number of cycles to liquefaction by a factor of approximately 2 to 3; however, the shape of the excess pore pressure response remains similar to the $D_r = 47\%$ tests. These relationships will be explored further in subsequent sections.

Pore pressure generation plots are presented in Figs. 4–7 for three uniform gravels: pea gravel, CLS8, and CLS5. Data for lower and upper bound values for clean sand from Lee and Albaisa (1974) are included in each figure for reference to typical sand pore pressure generation responses. Data from Evans and Seed (1987) for gravels are also included in some of the figures for comparison.

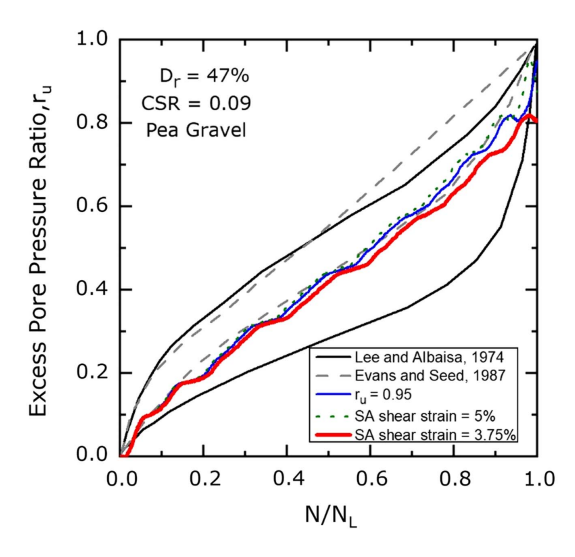


Fig. 3. Comparison of liquefaction definition on excess pore pressure generation ratio versus N/N_L .

Effect of Liquefaction Definition

Fig. 3 presents pore pressure generation data for pea gravel at $D_r = 47\%$, CSR = 0.09, and initial vertical stress of 100 kPa. Different liquefaction criteria were used on the same test data to explore the effect of the liquefaction definition on excess pore pressure generation response. The definition used throughout this paper and in most cyclic simple shear studies (Vaid and Sivathayalan 1996; Sivathayalan 2000; Porcino and Diano 2016) is that liquefaction occurs once the single amplitude (SA) shear strain reaches a level of 3.75%. This was compared to liquefaction definitions of SA shear strain of 5% and $r_u = 0.95$. Fig. 2 shows that the r_u values for the uniform gravels often did not reach a value of 1.0 and their values at SA = 3.75% could be as low as $r_u = 0.8$. Nonetheless, Fig. 3 shows that changing the definition of liquefaction has very

little effect on the r_u versus N/N_L relationship for pea gravel. The varying definitions all fall within a narrow range of response; therefore, the definition of SA = 3.75% was used in this study. For reference and comparison, the Lee and Albaisa (1974) and Evans and Seed (1987) predictive relationships for excess pore pressure generation are included in Fig. 3.

Effect of Particle Angularity

The effect of particle angularity on pore pressure response is shown in Fig. 4 for pea gravel, CLS5, and CLS8 at $D_r = 47\%$ and $D_r = 87\%$ and at initial vertical stresses ranging from 100 to 400 kPa. Figs. 4(a, b, and c) plot the excess pore pressure ratio versus the N/N_L value for each gravel at $D_r = 47\%$, and comparisons are

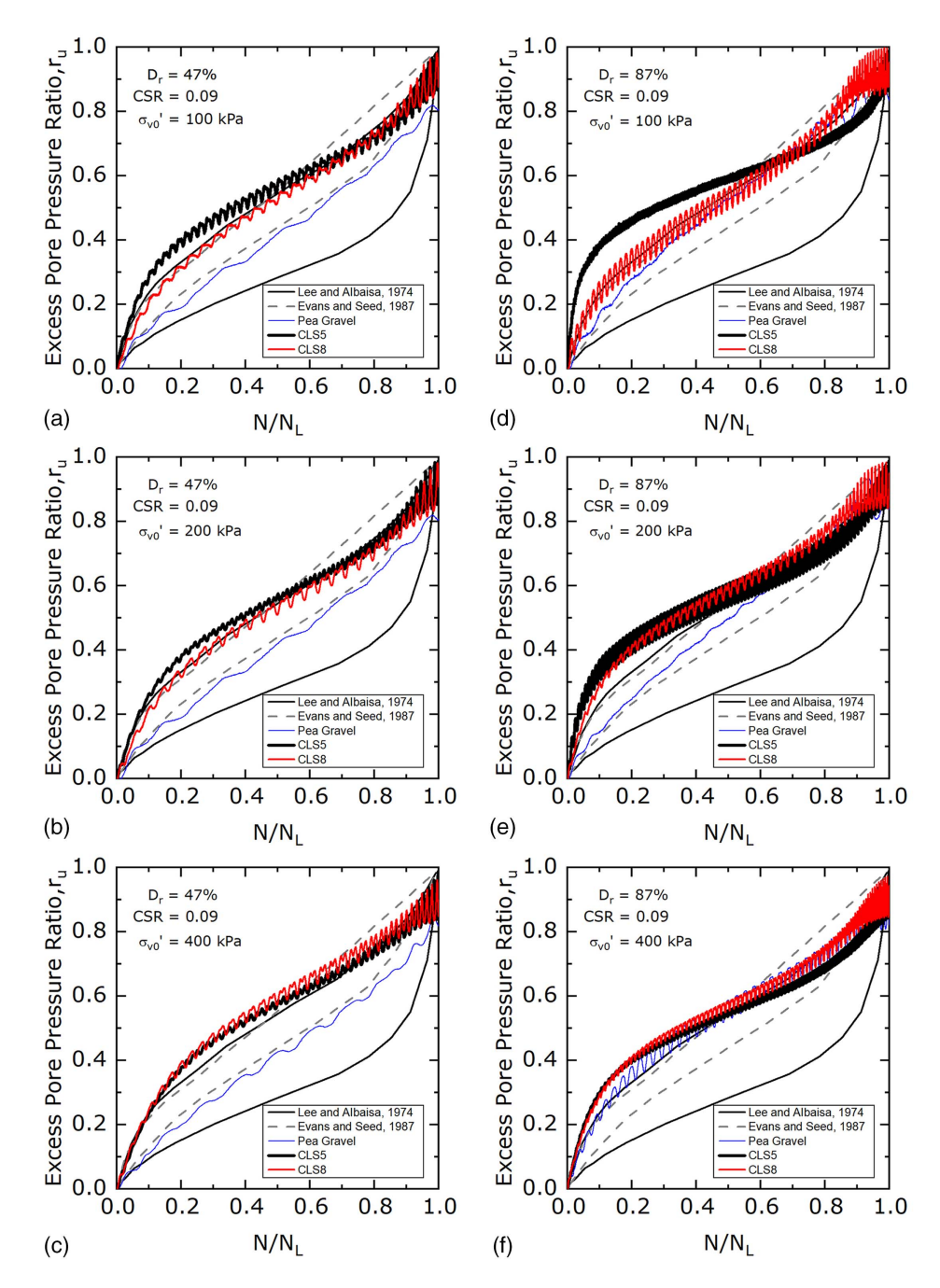


Fig. 4. Excess pore pressure ratio versus N/N_L for pea gravel, CLS5, and CL8 at CSR = 0.09 and $D_r = 47\%$ at (a) $\sigma'_{vo} = 100$ kPa; (b) $\sigma'_{vo} = 200$ kPa; and (c) $\sigma'_{vo} = 400$ kPa; and $D_r = 87\%$ at (d) $\sigma'_{vo} = 100$ kPa; (e) $\sigma'_{vo} = 200$ kPa; and (f) $\sigma'_{vo} = 400$ kPa.

made with Lee and Albaisa (1974) and Evans and Seed (1987). At a constant D_r , as particle angularity increases, a greater r_u is observed throughout the test. Specifically, at lower values of N/N_L (less than 0.4), the angular CLS materials generate greater pore pressure than the subrounded pea gravel. As vertical stress increases, the difference in r_{μ} remains essentially the same, with the pea gravel falling in the middle of the Lee and Albaisa (1974) data and the CLS materials falling near or slightly above the Lee and Albaisa (1974) and Evans and Seed (1987) upper bounds. Increasing D_r has a significant effect on particle angularity, as shown in Figs. 4(d, e, and f), which plot excess pore pressure ratio versus N/N_L for $D_r =$ 87% gravels. These plots show that, as D_r increases, the effect of particle angularity diminishes. The data for pea gravel, CLS5, and CLS8 now exhibit similar pore pressure generation that falls near the upper bound of Lee and Albaisa (1974) and Evans and Seed (1987). Furthermore, there are some differences in response at lower values of N/N_L (less 0.4) for the 100 and 200 kPa specimens, with the angular CLS materials falling marginally above the pea gravel. However, these differences diminish with increasing vertical stress, as evidenced by the similar response of all gravels, regardless of particle angularity, at 400 kPa.

Effect of Relative Density

The effect of relative density on pore pressure generation of uniform gravels is explored in Fig. 5. Figs. 5(a-c) illustrate the excess pore pressure generation versus the number of cycles at an initial vertical stress of 100 kPa and CSR = 0.09 for pea gravel, CLS5,

and CLS8, respectively. The test results show that, as relative density increases from $D_r = 47\%$ to $D_r = 87\%$, pore pressures accumulate at a slower pace for the angular CLS materials. It is expected that, as D_r increases, the number of cycles to liquefaction will increase and pore pressures will be generated at a slower pace. This response was observed for the angular CLS gravels but not the pea gravel. The pea gravel at $D_r = 47\%$ and $D_r = 87\%$ have similar responses, with the denser specimen sustaining a few more cycles before liquefaction. Figs. 5(d, e, and f) illustrate the data in normalized form using N/N_L . Fig. 5(d) shows that the pea gravel pore pressure generation response falls in the same range as the sands tested by Lee and Albaisa (1974). As the D_r increased from 47% to 87% there was a more abrupt increase in pore pressure generation as a function of N/N_L for the denser specimen that fell near the upper bound for sands. For the CLS materials [Figs. 5(e and f)] there was no observable pronounced change in pore pressure generation with increasing density; however, both the loose and dense specimens fall along the upper bound for sands found by Lee and Albaisa (1974).

Effect of Initial Vertical Effective Stress

Pore pressure generation plots for pea gravel, CLS5, and CLS8 at varying levels of initial vertical stress are shown in Fig. 6. The initial vertical stress ranged from 50 to 400 kPa for each gravel material at $D_r = 47\%$. Figs. 6(a-c) illustrate the excess pore pressure ratio versus the number of cycles to liquefaction at a CSR = 0.09. Fig. 6(a) shows that for the pea gravel material, as

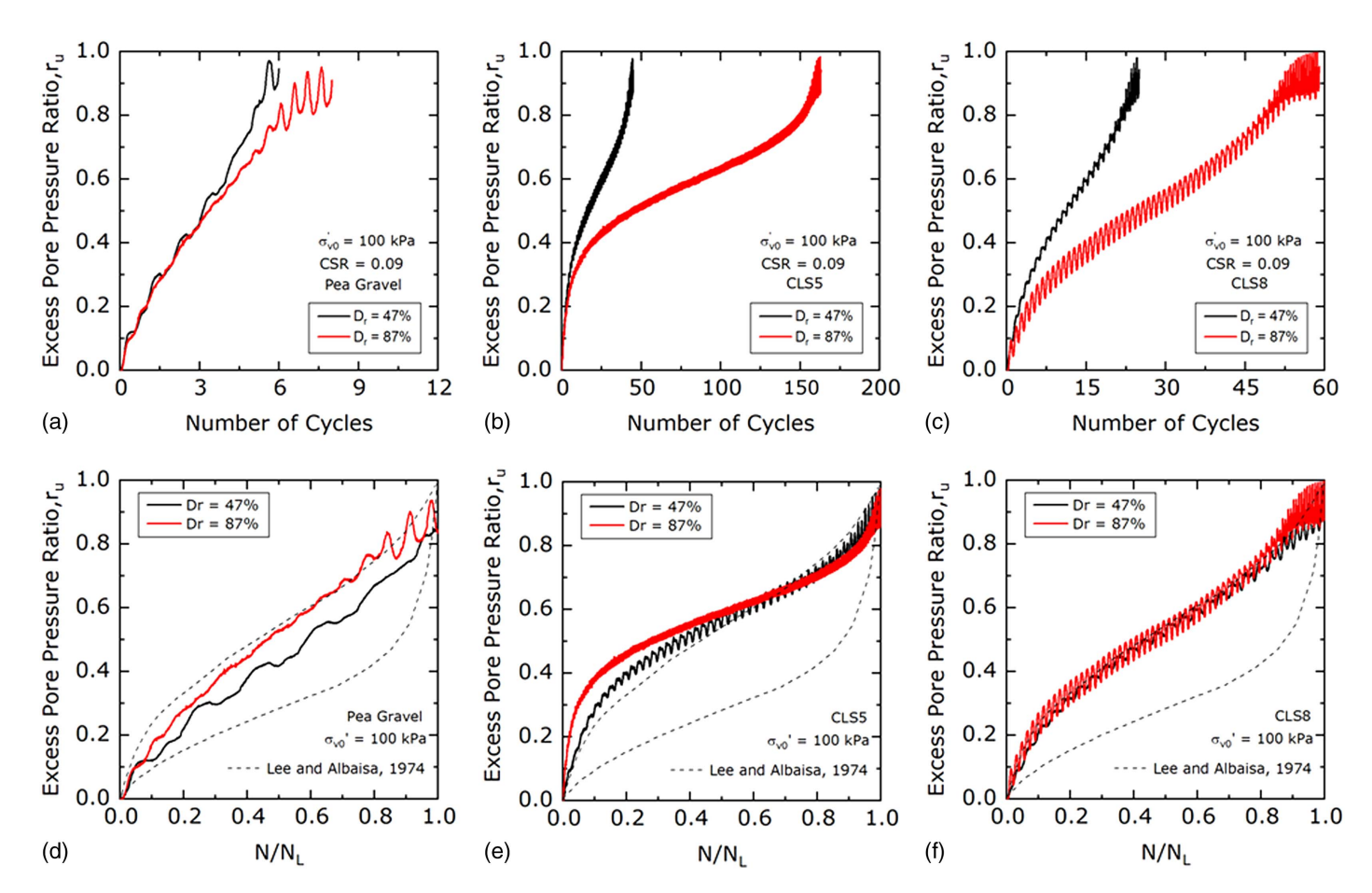


Fig. 5. Excess pore pressure ratio versus number of cycles at $\sigma'_{vo} = 100$ kPa, CSR = 0.09 for (a) pea gravel; (b) CLS5; and (c) CLS8 at $D_r = 47\%$ and $D_r = 87\%$; and excess pore pressure ratio versus N/N_L at $\sigma'_{vo} = 100$ kPa, CSR = 0.09 for (d) Pea Gravel; (e) CLS5; and (f) CLS8 at $D_r = 47\%$ and $D_r = 87\%$.

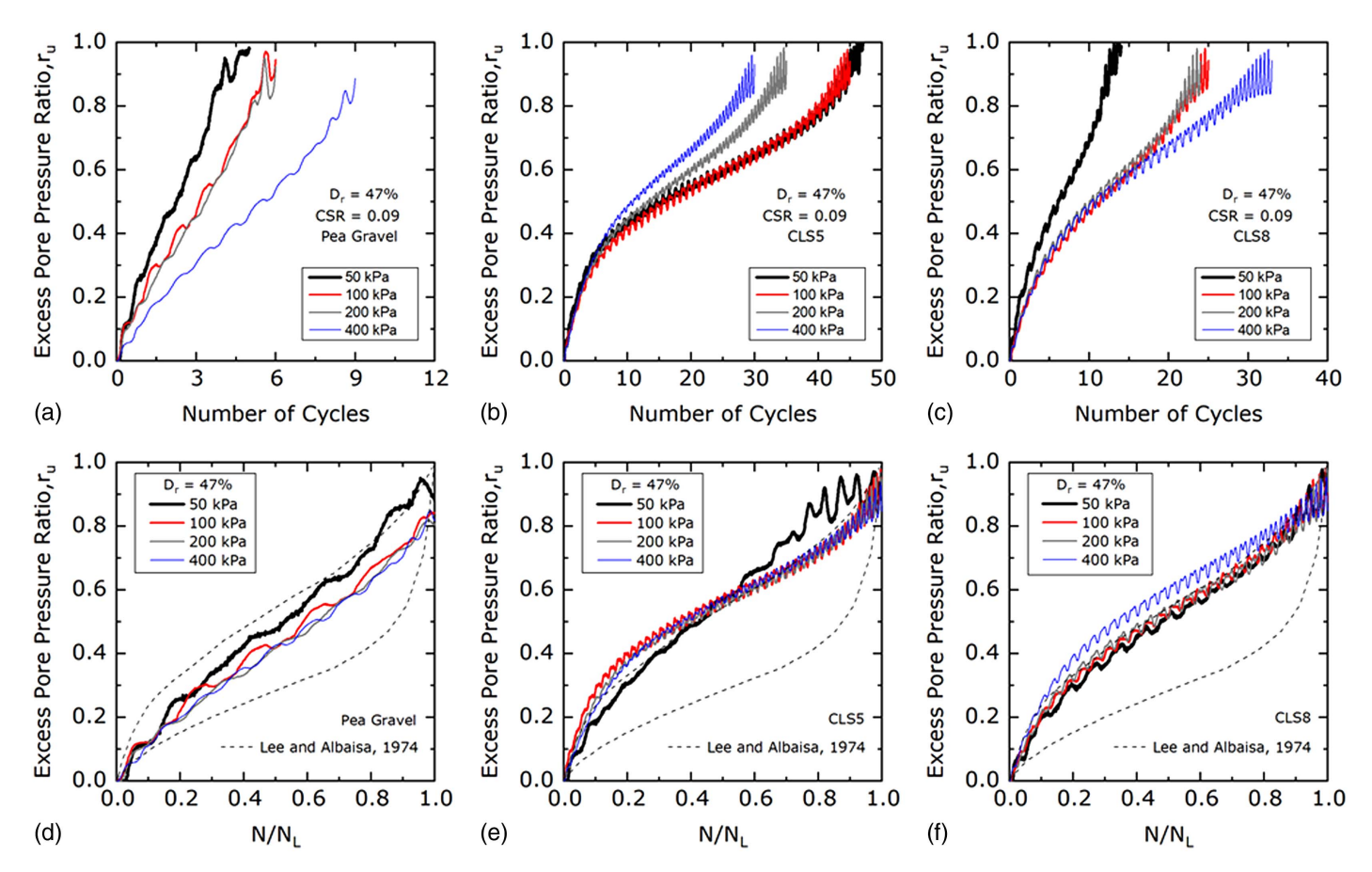


Fig. 6. Excess pore pressure ratio versus number of cycles at $D_r = 47\%$, CSR = 0.09 for (a) pea gravel; (b) CLS5; and (c) CLS8 at $\sigma'_{vo} = 50$ –400 kPa; and excess pore pressure ratio versus N/N_L at $D_r = 47\%$, CSR = 0.09 for (d) pea gravel; (e) CLS5; and (f) CLS8 at $\sigma'_{vo} = 50$ –400 kPa.

initial vertical stress increased, the number of cycles to liquefaction increased. Similar results were observed for the CLS8 material [Fig. 6(c)]. Fig. 6(b) shows that CLS5 material displayed a different response with increasing initial vertical stress: As the initial vertical stress increased, the number of cycles to liquefaction decreased. It is possible that the higher vertical stresses for this material induced some slight particle crushing that led to this trend.

Figs. 6(d, e, and f) plot the excess pore pressure ratio versus the N/N_L ratio. These figures show that initial vertical stress does not have a significant effect on pore pressure generation for the uniform gravel materials. This has also been shown for sands in previous studies (Polito et al. 2008). Comparison of the uniform gravels with the Lee and Albaisa (1974) data shows that the subrounded pea gravel data fall in the middle of the data range, while the angular CLS8 and CLS5 fall near the upper bound of the Lee and Albaisa (1974) data, highlighting the effect of particle angularity on pore pressure generation.

Effect of CSR

Fig. 7 compares the pore pressure generation response for uniform gravels at CSR = 0.04, 0.09, and 0.14 at $D_r = 47\%$ and initial vertical stress of 100 kPa. Figs. 7(a–c) plot the excess pore pressure ratio versus the number of cycles to liquefaction for the three uniform gravels. Fig. 7(a) plots the pea gravel response and shows that there is a significant difference in pore pressure generation for CSR = 0.04, compared to CSR = 0.09 and CSR = 0.14. The CSR = 0.04 specimen took approximately 240 cycles to liquefy,

while the CSR = 0.09 and CSR = 0.14 specimens each took six cycles to liquefy. Figs. 7(b and c) illustrate the response of CLS5 and CLS8 gravels at CSR = 0.09 and CSR = 0.14. CSR = 0.04 was not included in this case because the specimens did not liquefy at 500 cycles, which was the upper limit of testing. Nonetheless, Figs. 7(b and c) show that as CSR increases from 0.09 to 0.14 there is a significant decrease in the number of cycles to liquefaction and different pore pressure generation responses.

Figs. 7(d, e, and f) plot the excess pore pressure ratio versus the N/N_L ratio. These figures illustrate that CSR does not have a significant effect on pore pressure generation for the uniform gravel materials. For the pea gravel in Fig. 7(d), there is a slight change with CSR, with the CSR = 0.14 specimen showing slightly lower pore pressure generation; however, this difference is small and without further testing these responses should be considered similar. Results for the angular gravels, CLS5 and CLS8 [Figs. 7(e and f)] show that the response is practically the same for CSR = 0.14 and CSR = 0.09. Other authors (Polito et al. 2008) have similarly found that CSR does not have a significant effect on excess pore pressure generation values for sandy soils.

Effect of Sand Percentage

Mixtures of pea gravel with Ottawa C109 sand and CLS8 with Ottawa C109 sand were tested at different relative densities to evaluate the effect of varying sand percentage on the pore pressure generation of gravel-sand mixtures. Ottawa C109 sand is subrounded and has a $D_{50} = 0.35$ mm. Fig. 8 plots pea gravel

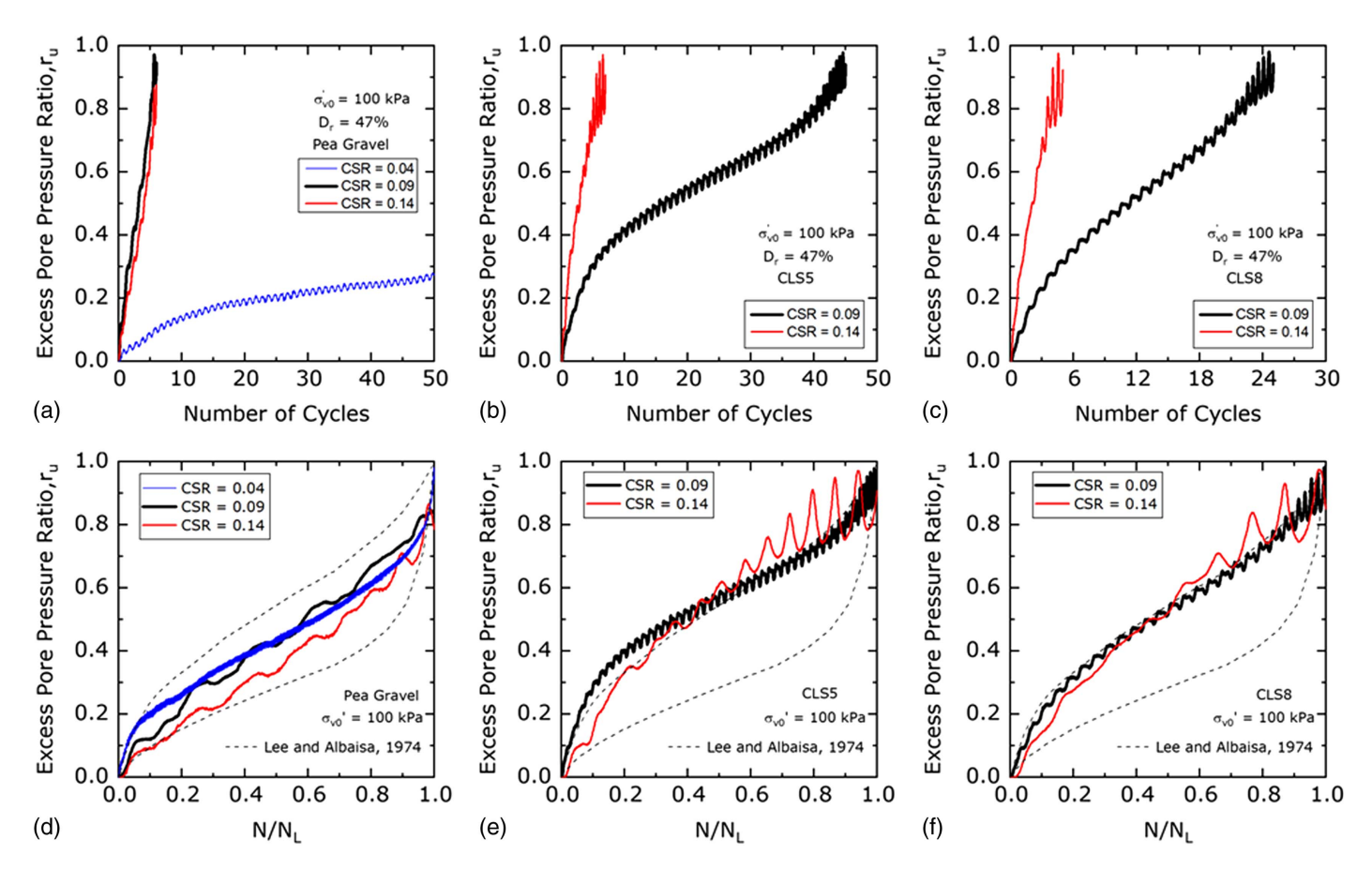


Fig. 7. Excess pore pressure ratio versus number of cycles at $D_r = 47\%$, $\sigma'_{vo} = 100$ kPa for (a) pea gravel (axis adjusted to 50 cycles; CSR = 0.04 exceeded 200 cycles); (b) CLS5; and (c) CLS8 at CSR = 0.04–0.14; and excess pore pressure ratio versus N/N_L at $D_r = 47\%$, $\sigma'_{vo} = 100$ kPa for (d) pea gravel; (e) CLS5; and (f) CLS8 at CSR = 0.04–0.14.

mixtures with sand percentages of 100%, 80%, 60%, 40%, and 0% at an initial vertical stress of 100 kPa at loose and dense states. Fig. 8(a) illustrates the excess pore pressure generation versus number of cycles to liquefaction for $D_r = 47\%$ specimens. The test data shows that the pore pressure response of the mixtures is different than the 100% sand or the 100% pea gravel. A 60% pea gravel and 40% sand mixture took 12 more cycles to liquefy than did the 60% sand/40% gravel specimen. The 40% sand/60% gravel specimen had the lowest void ratio, as discussed previously. The 100% sand and 100% pea gravel specimens liquefied in a similar number of cycles and generated pore pressures at a similar rate. This suggests that particle size may not play a significant role in pore pressure generation of uniform soils and that particle angularity governs the response as these two materials are subrounded. Fig. 8(c) illustrates the data from Fig. 8(a) as a function of the normalized ratio of N/N_L . The pea gravel/Ottawa sand mixtures all fall in a similar range that is within the middle to upper portion of the Lee and Albaisa (1974) data. Fig. 8(b) plots the same pea gravel mixtures at $D_r = 87\%$ at an initial vertical stress of 100 kPa. The increasing relative density had a significant effect only on the pore pressure generation of the 100% sand specimen, which took 187 cycles to liquefy. This suggests that for gap-graded gravel mixtures and uniform gravels, the effect of increasing density is not as significant as it is for sands. Fig. 8(d) plots r_u versus the normalized N/N_L ratio for the $D_r = 87\%$ gravel mixtures. The results show that increasing relative density does have an effect for the gravel mixtures as they now fall on the upper bound of the Lee and Albaisa (1974) relationship. The 100% sand specimen falls in the middle of the relationship and displays a different response than the dense gravel-sand mixtures. Overall, the gravel and sand mixtures respond similarly to the uniform gravel in both the loose state and dense state when compared based on the relationship between r_u and the normalized N/N_I .

Fig. 9 plots CLS8 mixtures with sand percentages of 100%, 80%, 60%, and 0% at an initial vertical stress of 100 kPa. Fig. 9(a) plots the excess pore pressure generation versus number of cycles to liquefaction for $D_r = 47\%$ specimens. The test data shows a different response for the angular CLS8 gravel mixtures than for the subrounded pea gravel mixtures. The angular CLS8 (100%) gravel required a significantly larger number of cycles to liquefy than did the Ottawa sand, which leads to the mixtures responding differently with the addition of gravel. The 80% sand mixture displayed a nearly identical response to the 100% sand mixture, indicating that the gravel is floating within the sand matrix and not contributing to cyclic shear resistance. The 60% sand mixture, which had the lowest void ratio, took 36 cycles to liquefy, which was greater than the 100% sand, 100% gravel, and 80% sand mixture. Fig. 9(c) plots the data from Fig. 9(a), but with the normalized ratio of N/N_L . The CLS8/Ottawa sand mixtures all fall in a similar range that is near the upper bound of the Lee and Albaisa (1974) data. Fig. 9(b) plots the same CLS8 mixtures at a $D_r = 87\%$ at initial vertical stress of 100 kPa. The results show that increasing the relative density only had a significant effect on the 100% sand and 100% gravel materials pore pressure generation. This response was slightly different than the pea gravel mixtures, because the CLS8 gravel is angular and required an increase in the number of

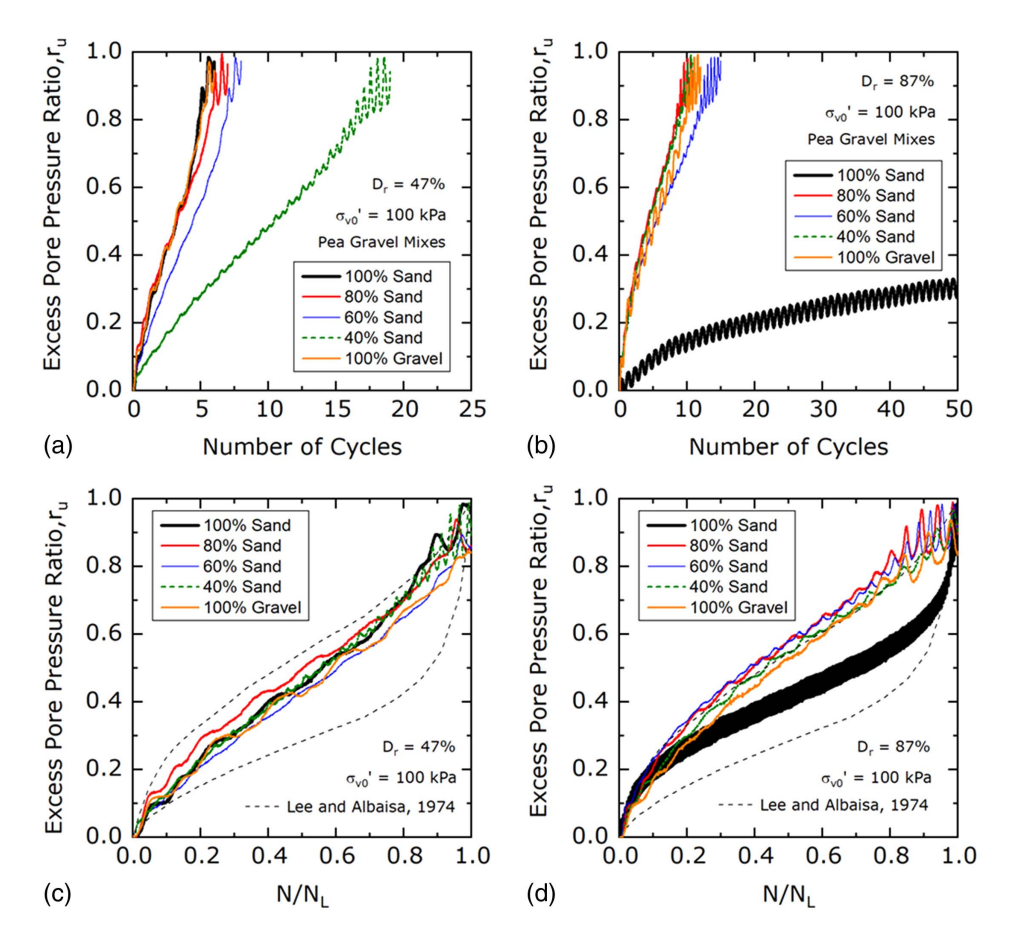


Fig. 8. Excess pore pressure generation versus number of cycles for pea gravel mixtures at (a) $D_r = 47\%$; and (b) $D_r = 87\%$ (axis adjusted to 50 cycles; 100% sand exceeded 200 cycles); and excess pore pressure generation versus N/N_L for pea gravel mixtures at (c) $D_r = 47\%$; and (d) $D_r = 87\%$.

cycles to liquefaction with increasing relative density, unlike the subrounded pea gravel. Interestingly, the inclusion of only 20% gravel (80% sand) in the specimen caused the specimen to liquefy in only 12 cycles, which was similar to the $D_r = 47\%$ specimen. Because the $D_r = 47\%$ specimens of 100% sand and 80% sand responded nearly identically, one might predict that the $D_r = 87\%$ specimens would respond similarly. It is possible that the 80% sand specimen at $D_r = 87\%$ responds similar to a $D_r = 47\%$ specimen with 80% sand because the specimen preparation method for the dense specimens is only compacting the gravel while the sand remains relatively loose. Fig. 9(d) plots r_u versus the normalized N/N_L ratio for the $D_r = 87\%$ gravel mixtures. The results show that the $D_r = 87\%$ mixed crushed limestone gravel specimens fall along the upper bound of the Lee and Albaisa (1974) relationship, but deviate from the 100% sand in a manner similar to the observed behavior of the dense mixed pea gravel specimens.

Comparison with Existing Relationships

Excess pore pressure generation upper and lower bound curves for soil materials ranging from sand (Lee and Albaisa 1974) and sand-silt mixtures (Porcino and Diano 2016) to gravels (Banerjee et al. 1979; Evans and Seed 1987; Hynes 1988; Haeri and Shakeri 2010) are shown in Fig. 10 along with data from this study for gravel and gravel-sand mixtures. Cyclic simple shear data from this study for uniform gravels and gravel-sand mixtures exhibited a pore pressure generation response close to the Evans and Seed (1987) data. The lower bound of excess pore pressure generation from this study is

approximately the mid-range of Lee and Albaisa (1974) for sands, while the upper bound from this study falls above the upper bound of Lee and Albaisa (1974). Excess pore pressure generation data was used to derive α values in Eq. (1) (Seed et al. 1975) for the gravel and gravel-sand mixtures. The α values for the lower bound and upper bound were 0.7 and 2.1, respectively. There was deviation between the derived α value and the upper bound data in the $N/N_L = 0.80-1.0$ range, as some specimens exhibited large pore pressure fluctuations in this range. The data showed that excess pore pressures were greater than Hynes (1988) and fell near the Porcino and Diano (2016) upper bound when N/N_L was less than approximately 0.40. Above $N/N_L = 0.40$, the gravels tested were closer to the Evans and Seed (1987) upper bound. The Banerjee et al. (1979) and Haeri and Shakeri (2010) data had significantly higher upper bounds than the gravel and gravel-sand mixtures tested in this study. The Haeri and Shakeri (2010) lower bound fell near the upper bound from this study.

Combining this data shows that soil mixtures (both gravel-sand and silt-sand) can have a wide range of pore pressure generation responses that can be different from those that were previously recommended for sands. These differences may be explained by the gradation characteristics of the materials, as summarized in Table 2. As shown in Table 2, gravelly soils may have a wide range of coefficient of uniformity (C_u). The highest C_u reported in Table 2 is for Oroville gravel ($C_u = 47$) that was tested by Banerjee et al. (1979), and the next highest is Tehran alluvium ($C_u = 28$) that was tested by Haeri and Shakeri (2010). Folsom gravel, tested by Hynes (1988), had a C_u of 14, whereas the gravel tested by Evans and Seed (1987)

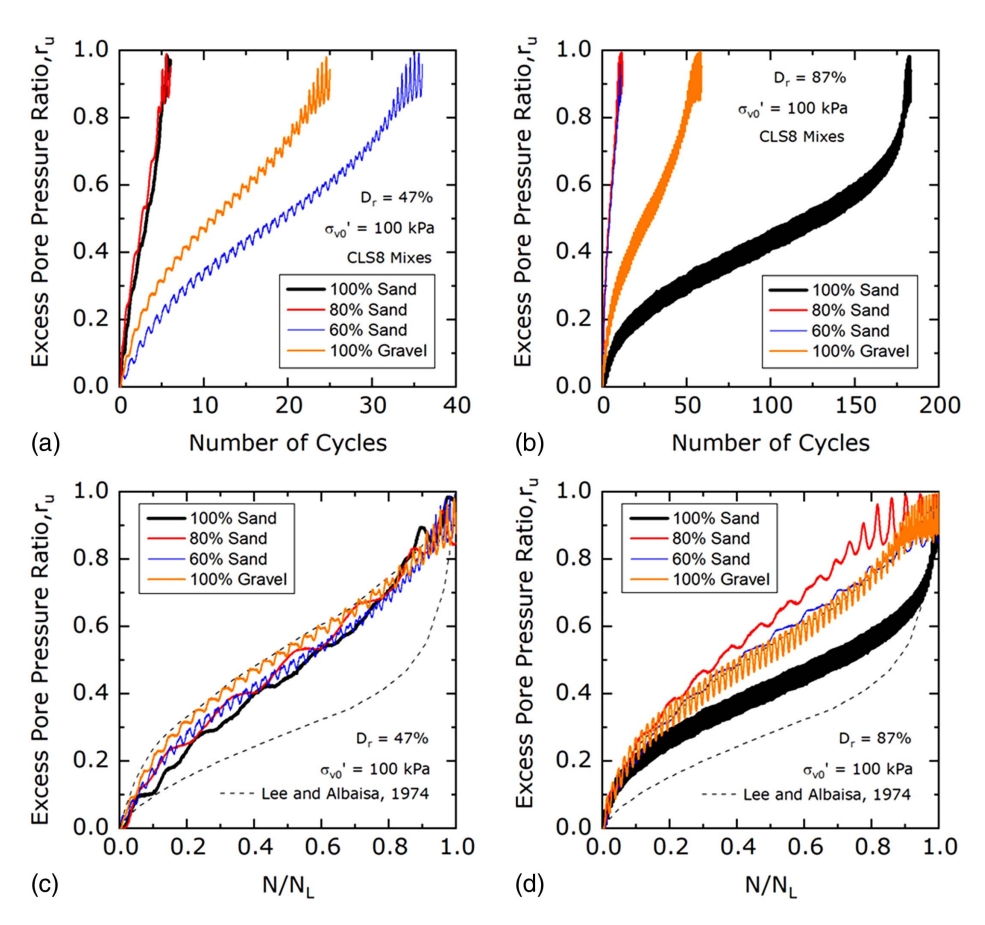


Fig. 9. Excess pore pressure generation versus number of cycles for CLS8 mixtures at (a) $D_r = 47\%$; and (b) $D_r = 87\%$; and excess pore pressure generation versus N/N_L for CLS8 mixtures at (c) $D_r = 47\%$; and (d) $D_r = 87\%$.

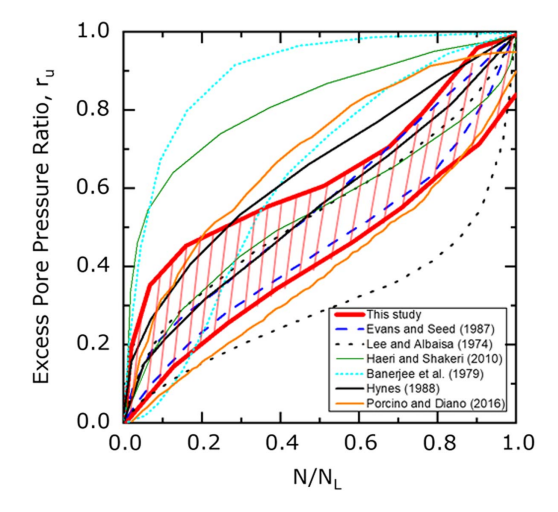


Fig. 10. Comparison of upper and lower bound values of excess pore pressure ratio versus N/N_L for materials from the literature and this study.

had a C_u of 1.3. The sand and silt mixtures tested by Porcino and Diano (2016) had C_u that ranged from 2.8 to 24. The uniform gravels in this study had $C_u < 2$, while the gravel-sand mixtures had C_u values up to 26. Fig. 11 illustrates the relationship between r_u and C_u at low $(N/N_L = 0.2)$, intermediate $(N/N_L = 0.5)$, and high $(N/N_L = 0.8)$ numbers of cycles prior to liquefaction. It shows that C_u , and by extension, gradation, has a significant effect on pore

pressure generation. As gravelly soils become more well-graded (higher C_u), their pore pressure generation increases rapidly in the first few cycles of loading and then flattens after reaching relatively high values of r_u in those first few cycles. These materials generally exhibit cyclic mobility and their pore pressure response reflects this behavior.

Effect of Gradation

As described earlier, Fig. 11 illustrates the relationship between the upper bound, average, and lower bound r_u and the coefficient of uniformity (C_u) at varying levels of N/N_L . The coefficient of curvature (C_c) was also evaluated, but the relationship between C_c and r_u was not as strong as that between C_u and r_u . The C_u data used in Fig. 11 is listed in Table 2 and includes gravel-sand mixtures from laboratory testing in this study as well from the literature, and sandsilt mixtures from the literature. Fig. 11 shows upper bound, average, and lower bound values for r_u at $N/N_L = 0.20$, 0.50, and 0.80. These values were chosen as representative of the r_u versus N/N_L curves presented in Fig. 10. The results show that at a lower value of N/N_L (i.e., $N/N_L=0.20$) there is a strong linear increase in r_u as C_u increases, and that the effect of increasing C_u diminishes as N/N_L increases. Equations were fitted to the data that estimate r_u based on C_u , as shown in Fig. 11. It should be noted that there were three points that were not consistent with the rest of the data for the upper bound and average values [as shown on Figs. 11(a and b) with full symbols] and this data was not included in the linear fit for upper bound and average values. These points were from the 60% pea gravel/40% Ottawa sand mixture that was

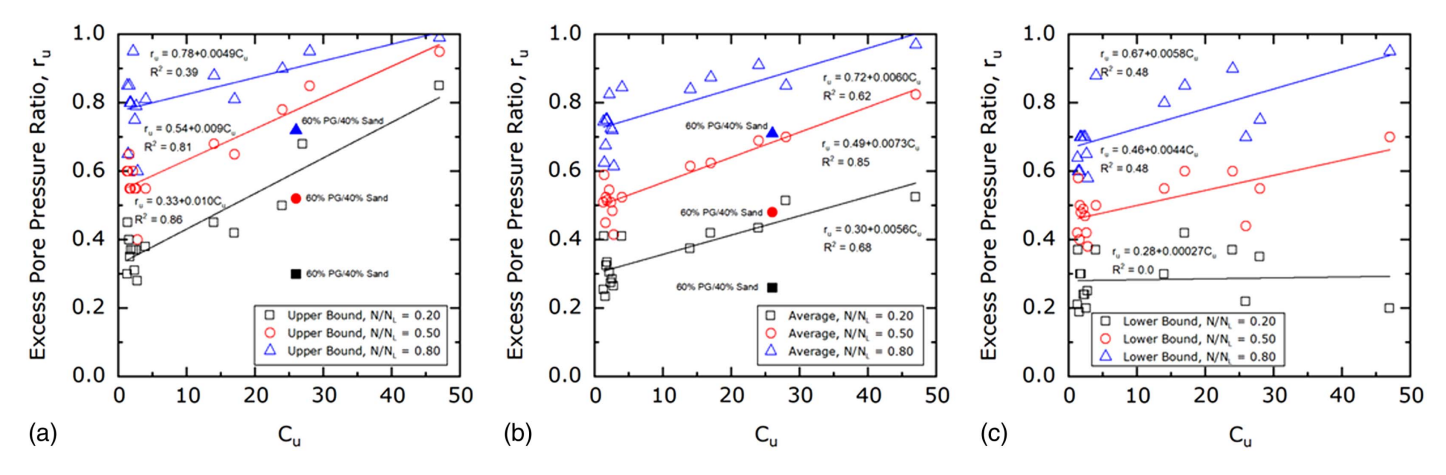


Fig. 11. Comparison of r_u versus C_u for (a) upper bound; (b) average; and (c) lower bound data.

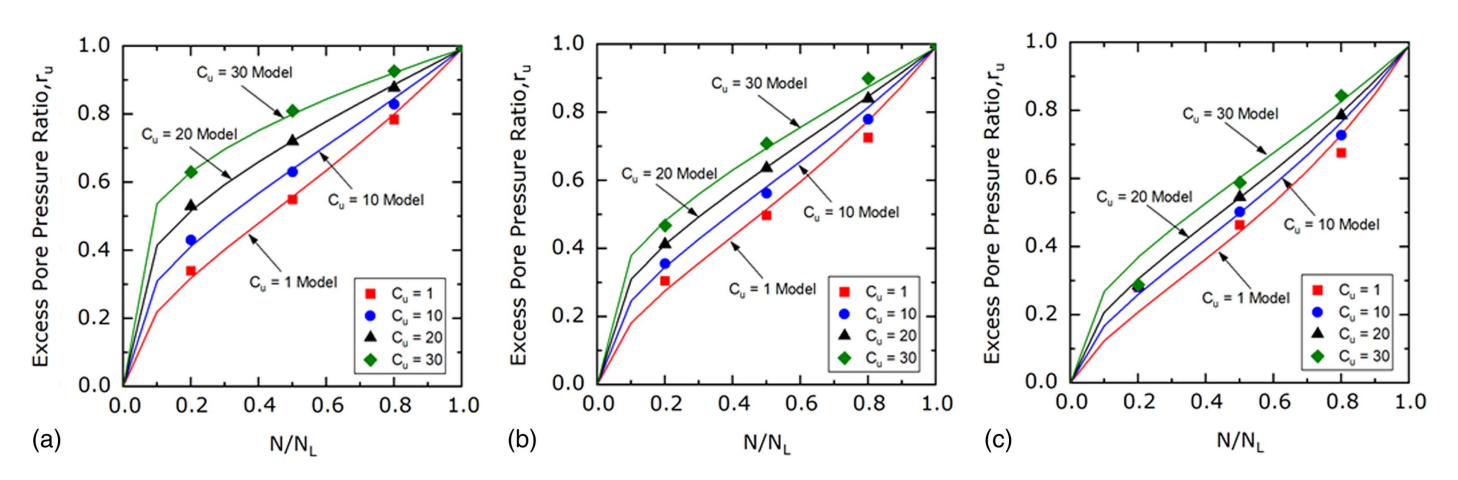


Fig. 12. Model Fit for $C_u = 1$, 10, 20, and 30 for (a) upper bound; (b) average; and (c) lower bound.

tested in this study. The 60% pea gravel/40% Ottawa sand mixture had a high value of C_u (26), but performed similarly to the 100% gravel specimen; therefore, it was not included in the relationship for C_u and r_u . This may be an indication that gap-graded soils with high values of C_u may not fit into the relationship, as these materials may resemble in response the larger or smaller fraction of the gap-graded mixture. This observation is of interest for gap-graded materials and requires further evaluation as more data are collected for gravelly soils.

The practical implication of the observation that r_u increases as C_u increases, specifically for $N/N_L=0.20$, is that well-graded materials can generate significant pore pressures in the early stages of cyclic shear that can have consequences on the induced shear strain and volumetric strain (i.e., settlement). Pore pressure development can also significantly alter seismic waves and amplification of sites during the liquefaction process (Zorapapel and Vucetic 1994).

Proposed C_u -Based Excess Pore Pressure Generation Model

Using the equations introduced in Fig. 11 that relate r_u at specific N/N_L values to C_u , a pore pressure model was developed to predict r_u . Values of $C_u=1,10,20$, and 30 were used with the equations from Fig. 11 for the upper bound, average, and lower bound for $N/N_L=0.20,\,0.50,\,$ and $0.80.\,$ A new equation that is similar in form to the Seed et al. (1975) model was found to provide the best fit to the data. The new equation is:

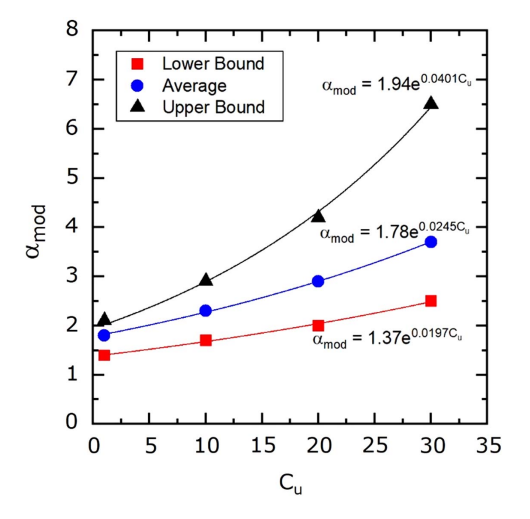


Fig. 13. Relationship of α_{mod} and C_u .

$$r_u = \frac{2}{\pi} \tan\left(\left(\frac{N}{N_L}\right)^{1/\alpha_{mod}}\right) \tag{3}$$

where α_{mod} is an empirical constant based on material properties and test conditions. Eq. (3) was used to fit the data points for $N/N_L=0.20,\,0.50,\,$ and 0.80 for $C_u=1,\,10,\,20,\,$ and 30 in Fig. 12 for the upper bound, average, and lower bound. The α_{mod} value was

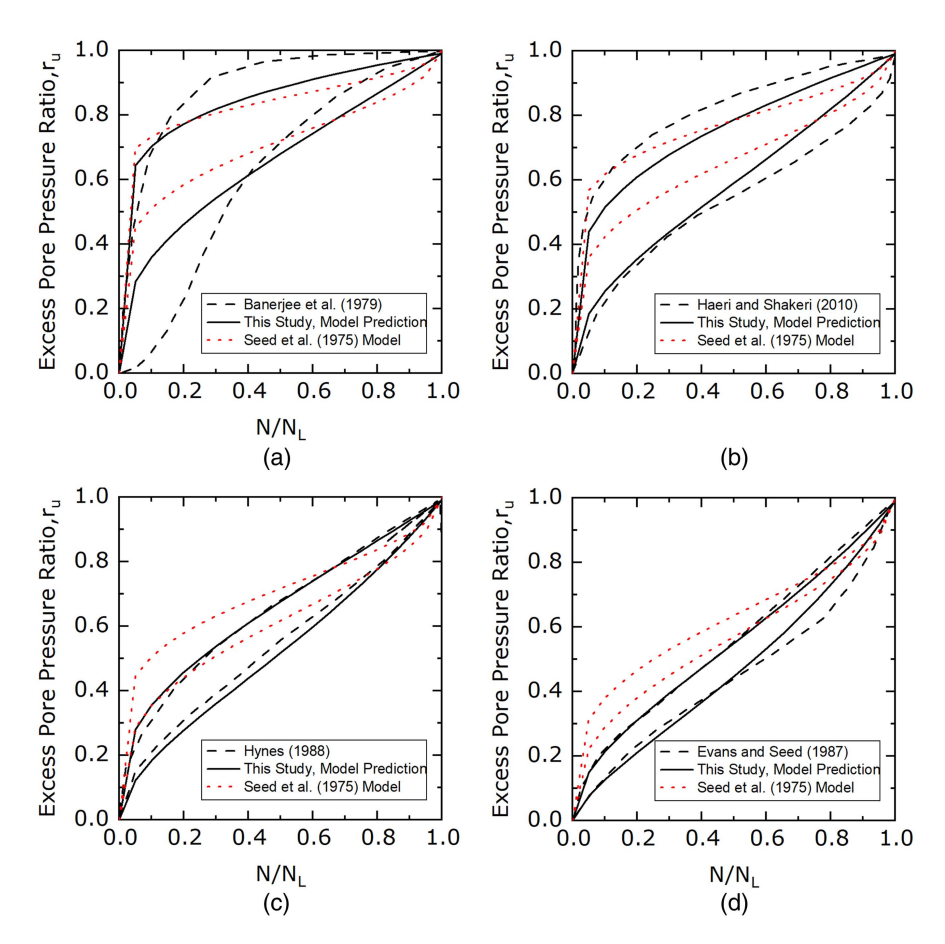


Fig. 14. Comparison of developed model with Seed et al. (1975) model and existing data for gravelly soils from (a) Banerjee et al. (1979); (b) Haeri and Shakeri (2010); (c) Hynes (1988); and (d) Evans and Seed (1987).

adjusted until a satisfactory fit was provided. These α_{mod} values for the upper bound, average, and lower bound for each C_u value are shown in Fig. 13, which provides a new method for predicting α_{mod} based on C_u for upper bound, average, and lower bound. The equations for finding α_{mod} for the model are:

Upper bound:

$$\alpha_{mod} = 1.94e^{0.0401C_u} \tag{4}$$

Average:

$$\alpha_{mod} = 1.78e^{0.0245C_u} \tag{5}$$

Lower bound:

$$\alpha_{mod} = 1.37e^{0.0197C_u} \tag{6}$$

These equations can be utilized to predict the α_{mod} value that should be used in Eq. (3) and highlight the influence of C_u on pore pressure generation.

Using this framework, comparisons were made with existing data for gravelly soils as well as the Seed et al. (1975) model in Fig. 14. For each comparison, Eqs. (4) and (6) were utilized to find the α_{mod} value for upper bound and lower bound based on the C_u value of the tested gravelly soil. This α_{mod} value was then inserted into Eq. (3). The α_{mod} values that were found using Eqs. (4) and (6) were also used for the Seed et al. (1975) model in place of α for comparison. Fig. 14(a) compares the model with Banerjee et al. (1979) data for $C_u=47$. The new pore pressure prediction model shows a satisfactory fit to the data that is improved compared to the

Seed et al. (1975) model. Fig. 14(b) compares the model with Haeri and Shakeri (2010) data for $C_u = 28$. The new pore pressure prediction model again shows a satisfactory fit to the data that is improved compared to the Seed et al. (1975) model. Fig. 14(c) compares the model with Hynes (1988) data for $C_u = 14$, while Fig. 14(d) compares the model with Evans and Seed (1987) data for $C_u = 1.3$. The new pore pressure prediction model fits the data very well for both Hynes (1988) and Evans and Seed (1987). Therefore, the new pore pressure prediction model is recommended for use with gravels and gravelly soils for prediction of excess pore pressure generation as a function of C_u . The Seed et al. (1975) model is still applicable for sands, which can have lower pore pressure generation than gravels. Predicting pore pressure generation is very important when assessing liquefaction potential for gravelly soils. The new pore pressure model provides a method to help further calibrate models used in numerical analyses and can also be used directly when advanced numerical analyses are not an option.

Conclusions

Excess pore pressure generation of uniform gravel and gravel-sand mixtures was evaluated in this study and it was found that uniform gravels and gravel-sand mixtures can exhibit different excess pore pressure generation responses than sands. Comparisons were made with existing relationships for pore pressure generation for sands. The effects of particle angularity of gravel, particle size, liquefaction definition, relative density, initial vertical effective stress, cyclic stress ratio, and gravel percentage for gravel-sand mixtures on the generation of excess pore water pressure were studied.

A new pore pressure model for gravelly soils was developed. The main findings are as follows:

- Liquefaction definition (either strain-based or r_u-based) did not influence the excess pore pressure generation when plotted on a normalized figure (N/N_L) for uniform pea gravel.
- As relative density increased, excess pore pressures generated at a slower pace for uniform gravels and the specimens liquefied at a greater number of cycles. The pea gravel pore pressure generation response fell in the same range as the sands tested by Lee and Albaisa (1974). Pore pressure generation for denser specimens fell near the upper bound for sands. For the CLS materials, no significant change was observed in the pore pressure generation as density increased, and both the loose and dense specimens fell along the upper bound for sands from Lee and Albaisa (1974).
- Increasing initial vertical stress and CSR does not have a significant effect on pore pressure generation for the uniform gravel materials, similar to observations for sands (Polito et al. 2008).
- More angular soils experience greater r_u throughout the test. Specifically, at lower values of N/N_L (less than 0.4), the angular CLS materials generate greater pore pressures than the sub-rounded pea gravel.
- Changes in D_r significantly influence the role that particle angularity plays in excess pore pressure generation. All pea gravel/Ottawa sand mixtures fell in a similar range and within the middle to upper portion of the Lee and Albaisa (1974) data. An increase in r_u was observed as relative density increased. The CLS8/Ottawa sand mixtures all fell along the upper bound of Lee and Albaisa (1974). As relative density increased for the CLS8 mixtures, only a small increase in r_u was observed.
- Gradation plays a key role in pore pressure generation, and one of the parameters that describes this effect is the coefficient of uniformity Cu. The uniform gravels in this study had Cu values below 2, while the sand-gravel mixtures had Cu values up to 26. Well-graded gravelly soils have a rapid increase in pore pressure generation in the first few cycles of loading, reaching relatively high values of ru in the first few cycles compared to more uniform gravels. Well-graded soils generally exhibit cyclic mobility and their pore pressure response reflects this behavior. At low N/NL (i.e., N/NL = 0.20) there is a strong linear increase in ru with increasing Cu, but the role of Cu diminishes as specimens approach liquefaction (i.e., N/NL increases). Gap-graded soils may behave more like one of the uniform fractions of the soil mixture.
- A new pore pressure model was developed that utilizes C_u to predict r_u for gravels and gravelly soils. The influence of gradation is not captured by existing pore pressure generation models that were developed for sands (with low C_u). The Seed et al. (1975) model is still applicable for sands.

Data Availability Statement

All data, models, and code generated or used during the study appear in the published article.

Acknowledgments

This material is based upon work supported by the National Science Foundation Graduate Student Research Fellowship under Grant No. DGE 1256260, by the National Science Foundation CAREER

Grant No. 1351403, and by CMMI Grant No. 1663288. Any opinions, findings, and conclusions or recommendations expressed in this material are those of the authors and do not necessarily reflect the views of the National Science Foundation.

References

- ASTM. 2016. Standard test methods for minimum index density and unit weight of soils and calculation of relative density. ASTM D4254-16. West Conshohocken, PA: ASTM.
- ASTM. 2019. Standard test method for consolidated undrained cyclic direct simple shear test under constant volume with load control or displacement control. ASTM D8296-19. West Conshohocken, PA: ASTM.
- Banerjee, N. G., H. B. Seed, and C. K. Chan. 1979. Cyclic behavior of dense coarse-grained materials in relation to the seismic stability of dams. UBC/EERC-79-13. Berkeley, CA: Univ. of California.
- Belkhatir, M., T. Schanz, A. Arab, N. Della, and A. Kadri. 2014. "Insight into the effects of gradation on the pore pressure generation of sand–silt mixtures." *Geotech. Test. J.* 37 (5): 20130051. https://doi.org/10.1520/GTJ20130051.
- Berrill, J. B., and R. O. Davis. 1985. "Energy dissipation and seismic lique-faction of sands: Revised model." *Soils Found*. 25 (2): 106–118. https://doi.org/10.3208/sandf1972.25.2_106.
- Booker, J. R., M. S. Rahman, and H. B. Seed. 1976. *GADFLEA: A computer program for the analysis of pore pressure generation and dissipation during cyclic or earthquake loading*. UBC/EERC 76-24. Berkeley, CA: Univ. of California.
- Chang, W. J., C. W. Chang, and J. K. Zeng. 2014. "Liquefaction characteristics of gap-graded gravelly soils in K₀ condition." Soil Dyn. Earthquake Eng. 56 (Nov): 74–85. https://doi.org/10.1016/j.soildyn.2013.10.005.
- Cubrinovski, M., and K. Ishihara. 2002. "Maximum and minimum void ratio characteristics of sands." Soils Found. 42 (6): 65–78. https://doi.org/10.3208/sandf.42.6_65.
- Dash, H. K., and T. G. Sitharam. 2009. "Undrained cyclic pore pressure response of sand–silt mixtures: Effect of nonplastic fines and other parameters." Geotech. Geol. Eng. 27 (4): 501–517. https://doi.org/10 .1007/s10706-009-9252-5.
- De Alba, P., C. K. Chan, and H. B. Seed. 1975. Determination of soil liquefaction characteristics by large scale laboratory tests. UBC/ EERC-75-14. Berkeley, CA: Univ. of California.
- Dobry, R., R. S. Ladd, F. Y. Yokel, R. M. Chung, and D. Powell. 1982.
 Prediction of pore water pressure buildup and liquefaction of sands during earthquake by the cyclic strain method. Gaithersburg, MD: National Bureau of Standards.
- Dobry, R., W. G. Pierce, R. Dyvik, G. E. Thomas, and R. S. Ladd. 1985. *Pore pressure model for cyclic straining of sand*. Research Rep. No. CE-85. New York: Rensselaer Polytechnic Institute.
- Dyvik, R., T. Berre, S. Lacasse, and B. Raadim. 1987. "Comparison of truly undrained and constant volume direct simple shear tests." *Geotechnique* 37 (1): 3–10. https://doi.org/10.1680/geot.1987.37.1.3.
- Evans, M. D., and H. B. Seed. 1987. *Undrained cyclic triaxial testing of gravels—The effect of membrane compliance*. UCB/EERC-87/08. Berkeley, CA: Univ. of California.
- Evans, M. D., and S. Zhou. 1995. "Liquefaction behavior of sand-gravel composites." *J. Geotech. Eng.* 121 (3): 287–298. https://doi.org/10.1061/(ASCE)0733-9410(1995)121:3(287).
- Fragaszy, R. J., and S. Sneider. 1991. "Compaction control of granular soils: Final report." Research Project GC 8720, Task 08. Washington, DC: Department of Transportation, Planning, Research and Public Transportation Division.
- Green, R. A., J. K. Mitchell, and C. P. Polito. 2000. "An energy-based excess pore pressure generation model for cohesionless soils." In Proc., The John Booker Memorial Symp.—Developments in Theoretical Geomechanics, 383–390. Rotterdam, Netherlands: A.A. Balkema.
- Haeri, S. M., and M. R. Shakeri. 2010. "Effects of membrane compliance on pore water pressure generation in gravelly sands under cyclic loading." *Geotech. Test. J.* 33 (5): 375–384. https://doi.org/10.1520/GTJ102433.

- Hubler, J. F., A. Athanasopoulos-Zekkos, and D. Zekkos. 2017a. "Monotonic, cyclic, and postcyclic simple shear response of three uniform gravels in constant volume conditions." *J. Geotech. Geoenviron. Eng.* 143 (9): 04017043. https://doi.org/10.1061/(ASCE)GT.1943-5606.0001723.
- Hubler, J. F., A. Athanasopoulos-Zekkos, and D. Zekkos. 2017b. "Pore pressure generation of pea gravel, sand, and gravel-sand mixtures in constant volume simple shear." In Proc., 3rd Int. Conf. on Performance-based Design in Earthquake Geotechnical Engineering (PBD-III). Vancouver, BC, Canada: International Society of Soil Mechanics and Geotechnical Engineering.
- Hubler, J. F., A. Athanasopoulos-Zekkos, and D. Zekkos. 2018. "Monotonic and cyclic simple shear response of gravel-sand mixtures." Soil Dyn. Earthquake Eng. 115 (11): 291–304. https://doi.org/10.1016/j.soildyn.2018.07.016.
- Hynes, M. E. 1988. "Pore pressure generation characteristics of gravel under undrained cyclic loading." Ph.D. thesis, Dept. of Civil Engineering, Univ. of California.
- Kammerer, A. M., J. Wu, M. F. Riemer, J. M. Pestana, and R. B. Seed. 2004. "A new multi-directional direct simple shear testing database." In *Proc.*, 13th World Conf. on Earthquake Engineering. Tokyo: International Association for Earthquake Engineering.
- Kokusho, T. 2013. "Liquefaction potential evaluations: Energy-based method versus stress-based method." Can. Geotech. J. 50 (10): 1088–1099. https://doi.org/10.1139/cgj-2012-0456.
- Lade, P. V., C. D. Liggio, and J. A. Yamamuro. 1998. "Effects of non-plastic fines on minimum and maximum void ratios of sand." ASTM Geotech. Test. J. 21 (4): 336–347. https://doi.org/10.1520/GTJ11373J.
- Lee, K. L., and A. Albaisa. 1974. "Earthquake induced settlements in saturated sands." J. Geotech. Geoenviron. Eng. 100 (4): 387–406. https://doi.org/10.1061/AJGEB6.0000034.
- Martin, G. R., H. B. Seed, and W. D. L. Finn. 1975. "Fundamentals of liquefaction under cyclic loading." *J. Geotech. Eng. Div.* 101 (5): 423–438. https://doi.org/10.1061/AJGEB6.0000164.
- Mei, X., S. Olson, and Y. M. A. Hashash. 2018. "Empirical porewater pressure generation model parameters in 1-D seismic site response analysis." Soil Dyn. Earthquake Eng. 114 (7): 563–567. https://doi.org/10.1016/j.soildyn.2018.07.011.
- Polito, C. P. 1999. "The effects of non-plastic and plastic fines on the liquefaction of sandy soils." Doctoral dissertation, Dept. of Civil Engineering, Virginia Polytechnic Institute.

- Polito, C. P., R. A. Green, and J. Lee. 2008. "Pore pressure generation models for sands and silty soils subjected to cyclic loading." *J. Geotech. Geoenviron. Eng.* 134 (10): 1490–1500. https://doi.org/10.1061/(ASCE)1090-0241(2008)134:10(1490).
- Polito, C. P., and J. R. Martin. 2001. "Effects of nonplastic fines on the liquefaction resistance of sands." J. Geotech. Geoenviron. Eng. 127 (5): 408–415. https://doi.org/10.1061/(ASCE)1090-0241(2001) 127:5(408).
- Polito, C. P., and E. L. Sibley. 2020. "Threshold fines content and behavior of sands with nonplastic silts." *Can. Geotech. J.* 57 (3): 462–465. https://doi.org/10.1139/cgj-2018-0698.
- Porcino, D., and V. Diano. 2016. "Laboratory study on pore pressure generation and liquefaction of low-plasticity silty sandy soils during the 2012 earthquake in Italy." *J. Geotech. Geoenviron. Eng.* 142 (10): 04016048. https://doi.org/10.1061/(ASCE)GT.1943-5606.0001518.
- Seed, H. B., P. P. Martin, and J. Lysmer. 1975. The generation and dissipation of pore-water pressures during soil liquefaction. Berkeley, CA: Univ. of California.
- Sivathayalan, S. 2000. "Fabric, initial state and stress path effects on liquefaction susceptibility of sands." Ph.D. thesis, Dept. of Civil Engineering, Univ. of British Columbia.
- Vaid, Y. P., and S. Sivathayalan. 1996. "Static and cyclic liquefaction potential of Fraser Delta sand in simple shear and triaxial tests." Can. Geotech. J. 33 (2): 281–289. https://doi.org/10.1139/t96-007.
- Vucetic, M., and R. Dobry. 1986. Pore pressure build-up and liquefaction at level sandy sites during earthquakes. New York: Rensselaer Polytechnic Institute.
- Wong, R. T., H. B. Seed, and C. K. Chan. 1974. Liquefaction of gravelly soils under cyclic loading conditions. UCB/EERC-74/11. Berkeley, CA: Univ. of California.
- Wu, J., A. M. Kammerer, M. F. Riemer, R. B. Seed, and J. M. Pestana. 2004. "Laboratory study of liquefaction triggering criteria." In *Proc.*, 13th World Conf. on Earthquake Engineering. Vancouver, BC, Canada: International Association for Earthquake Engineering.
- Zekkos, D., A. Athanasopoulos-Zekkos, J. F. Hubler, X. Fei, K. Zehtab, and A. Marr. 2018. "Development of a large-size cyclic direct simple shear device for characterization of ground materials with oversized particles." *Geotech. Test. J.* 41 (2): 20160271. https://doi.org/10.1520/GTJ20160271.
- Zorapapel, G. B. T., and M. Vucetic. 1994. "The effects of seismic pore water pressure on ground surface motion." *Earthquake Spectra* 10 (2): 403–438. https://doi.org/10.1193/1.1585780.